Amido bisphosphonic acid as anchoring agent and photopolymerization initiator onto zirconium oxide surface

Jihen Ben-Hadj-Salem, Diana Dragoe, Philippe Marie, Sandrine Froissart, Arnaud Fouchet, Jacques Rouden, Jérôme Lecourt, Christelle Harnois, Soufiane Touil, Jérôme Baudoux, et al.

Version of Record: https://www.sciencedirect.com/science/article/pii/S0014305723003907
Manuscript_6a7723fa9a5c99abe1783d065d4f6679

Amido bisphosphonic acid as anchoring agent and photopolymerization initiator onto zirconium oxide surface

Jihen Ben-Hadj-Salem[a,b], Diana Dragoe[c], Philippe Marie[d], Sandrine Froissart[e], Arnaud Fouchet[e], Jacques Rouden[a], Jérôme Lecourt[e], Christelle Harnois[e], Soufiane Touil[b], Jérôme Baudoux[a], Bénédicte Lepoittevin[a*]

[a] Normandie Univ, ENSICAEN, UNICAEN, CNRS, Laboratoire de Chimie Moléculaire et Thio-organique (LCMT) UMR 6507, 6 Bd du Maréchal Juin, 14000 Caen, France

[b] Université de Carthage, Faculté des Sciences de Bizerte, Laboratoire des composés Hétéro-Organiques et Matériaux Nanostructurés (LR18ES11), Jarzouna 7021, Tunisie

[c] ICMMO, UMR CNRS 8182, Univ. Paris-Saclay, 91405 Orsay, France

[d] Normandie Univ, ENSICAEN, UNICAEN, CNRS, Centre de Recherche sur les Ions, les Matériaux et la Photonique (CIMAP), 6 Bd du Maréchal Juin, 14000 Caen, France

[e] NORMANDIE UNIV, ENSICAEN, UNICAEN, CNRS, CRISMAT, 14000 CAEN, FRANCE

Corresponding author. B. Lepoittevin benedicte.lepoittevin@ensicaen.fr

Abstract

The surface modification of metal oxides by grafting an organic molecule allows the development of new specific properties on demand. In this work, we demonstrate the modification of the Yttria Tetragonal Zirconia Polycrystal (Y-TZP), which is a ceramic widely used in dental implantology, by polymer grafting of the surface in a three-steps protocol for tuning the wetting properties. The first step involved the preparation of zirconia pellet by sintering followed by their surface activation. In the second step, the organic initiator bearing a tertiary amine such as the *N*,*N*-dimethylamino group capable of initiating a radical photopolymerization reaction, was grafted onto the surface through a bisphosphonic acid functionality. In the last step, two monomers, namely methyl methacrylate and styrene, were photopolymerized on the zirconia surface by blue light irradiation.

The chemical steps were monitored and characterized by X-ray photoelectron spectroscopy (XPS), spectroscopic ellipsometry (SE) and Atomic Force Microscopy (AFM). Wetting properties to different polar and nonpolar liquids and surface energies calculated with the Van Oss theory were found to vary systematically depending on the type of functionalization and grafting. This methodology is very promising for surface tuning of the dental ceramic.

Key words

Zirconia, hybrid materials, bisphosphonic acid, grafting from, free radical photopolymerization.

1. Introduction

In recent years, the use of ceramic for medical appplications has increased interest because of three factors: aesthetics, biocompatibility, and high mechanical toughness [1]. Particularly, the Yttria-stabilized Tetragonal Zirconia Polycrystal (Y-TZP) is used as the standard core material in ceramics for dental restorations. Implant technology has developed different methodologies to modify zirconia surface regarding biological properties (cell attachment, osseointegration, antibacterial properties…). However, although biocompatible, zirconia can lead to bacterial biocontamination. Therefore it is important to modifiy the surface of zirconia to tune their properties such as (anti)adhesion, lubrication, wettability, biocompatibility and antibacterial activity. In the literature, some authors have already explored different treatments to modify surface properties of zirconia [2-7].

In literature, there are different techniques to modify the surface: physical techniques (sandblasting, ultraviolet irradiation, laser application, plasma treatment) and chemical techniques (acid etching, dip-coating and self-assembled monolayers, hydrolysis, oxidation, layer-by-layer assembly and polymers grafting) [8-10]. The latter is particularly interesting because ultrathin grafted polymer layers can modulate the surface properties of different substrates without altering their bulk performance. In general, grafting a polymer can be done according to two main methods: the "grafting-to" technique which is based on the fixation of a polymer previously synthesized on the surface of a material, and the "grafting-from" technique where the polymerization is directly carried out by an initiator grafted on the surface. The “grafting to” approach suffers from less control due to steric hindrance on the surface whereas a better polymerization control (grafting densities, chain length) can be obtained using the “grafting-from” approach [11-13].

Indeed for “grafting from” polymerization on Y-TZP surface, an organic anchoring agent carrying a radical polymerization initiator group is needed. Various chemical groups can be grafted on inorganic surfaces: carboxylic acids, alcohols, amines, amides or silanes are the most often encountered ones [14]. Among these anchoring functions, phosphonic acids and derivatives have many advantages; we can highlight excellent complexing properties and chemical resistance [15]. Moreover, these functions very rarely lead to homocondensation and can be linked to various materials such as TiO_2 [16,17], ZrO_2 [16], Y_2O_3 [18], Fe_3O_4 [19] and perovskites ($BaTiO_3$) [20] by formation of P-O-M (M = Ti, Zr) bonds. A variety of studies proved the high stability of the P-O-M bonds under various conditions such as UV irradiation, thermal treatment or aqueous immersion at different pH values [21]. Combination of experiments performed by ^{31}P NMR MAS (magic angle spinning), ^{17}O NMR, ToF-SIMS and XPS demonstrated that phosphonic acids allow mono-, bi-, and tri-dentate binding modes associated with possible electrostatic and hydrogen-bonding interactions [14,22]. In addition, it was

previously shown that mono, bis and multifunctional phosphonic acids can be used for surface modification on metal oxides, their functionality allows to modulate the grafting densities [23].

To the best of our knowledge, very few examples reported the use of phosphonic acids as anchoring agents for polymer grafting on zirconia surface. Lomoschitz et al reported a covalent grafting of phosphorus-based coupling agents carrying a polymerizable methacrylate moiety on ZrO_2 nanoparticles, generating a highly functional surface [21]. Kickelbick et al described the preparation of polyester nanocomposite by attaching 3-phosphonopropionic acid to zirconia. Then, polycondensation reaction was performed in the presence of isophthalic acid and neopentyl glycol as monomers [24].

In this study, we will discuss the covalent grafting of a new versatile molecule carrying a bisphosphonic acid as anchoring group and a tertiary amine allowing the initiation of a radical photopolymerization reaction on Y-TZP, generating a highly functional surface. Although there are many methods for surface modification in literature, the methodology described in this publication may specifically target materials based on metal oxides.

2. Materials and methods

2.1. Materials

All starting reagents and solvents were commercially available and used without additional purification. Anhydrous solvents were obtained from a PURESOLV SPS400 apparatus developed by Innovative Technology Inc. (Hong Kong, China). Tosoh TZ-3YB-E zirconia powder (ZrO_2/Y_2O_3 97/3 mol%, particle size 40 nm) was purchased from Tosoh Europe. 4-Dimethylbenzoyl chloride, triethyl phosphite, formamide, phosphorus oxychloride, and camphorquinone were purchased from Sigma Aldrich. Bromotrimethylsilane (98 %), triethylamine (99 %) and sulfuric acid (96 %) were obtained from Acros organics. Methyl methacrylate (MMA, 99 %, Aldrich) and styrene (99 %, Aldrich) were passed through a basic alumina column to remove the polymerization inhibitor before use.

Photopolymerization reactions were made on 20 mL screw vials 24 mm clear glass from Interchim (CK1540) and in an Evolu Chem Photo RedOx Box Hepato Chem using blue led lamp (450 - 455 nm) purchased from Interchim. Camphorquinone photophysic characteristics are given in Table 1 [25].

Table 1. Redox potentials E_{ox}, E_{red}, triplet state E_T and singlet state E_s energy levels for camphorquinone photoinitiator [25].

E_{ox} (V)	E_{red} (V)	E_T (eV)	E_S (eV)
> 2	- 1.44	2.02	2.5

2.2. Characterizations

^{1}H, ^{13}C and ^{31}P NMR spectra were obtained on a Bruker 500 MHz Spectrometer. Deuterated solvents for solution NMR analysis were acquired from Euristop, Inc (chloroform and water) and Aldrich (NaOD).

Contact angles measurements were carried out by the Young-Laplace method using a DSA30 Krüss goniometer with high purity water (Millipore, milliQ). The static contact angle was measured within 5 s of placing the drop (1 µL) on the surfaces and an average of five measurements was reported.

Surface free energy values of Y-TZP samples with each step has been determined by measuring the contact angle of the three test liquids. Formamide (supplied by Aldrich) and diiodomethane (99 %, stabilized, Thermo-scientific) were used as a polar and nonpolar solvent, respectively.

The approach of Good, Van Oss and Chaudhury (acid-base theory) was used to calculate the surface free energy and energetic characteristic [26,27]. The surface energy δ_i is seen as the sum of a Lifshitz-van der Waals apolar component δ_i^{LW} and a Lewis acid-base polar component δ_i^{AB}:

$$\delta_i = \delta_i^{LW} + \delta_i^{AB} \quad (1)$$

The acid-base polar component δ_i^{AB} can be further subdivided by using specific terms for an electron donor (δ_i^{+}) and an electron acceptor (δ_i^{-}) subcomponent:

$$\delta_i^{AB} = 2(\delta_i^{+} \delta_i^{-})^{1/2} \quad (2)$$

The surface energy components of a surface (δ_S^{+}, δ_S^{-} and δ_S^{LW}) were determined by performing contact angle measurements with three liquids with known surface tension parameters (δ_L^{+}, δ_L^{-} and δ_L^{LW}). Using the Young equation, a relation between the measured contact angles (Θ), the liquid surface energy and the solid energy can be obtained.

$$\delta_L(1+\cos\Theta) = 2((\delta_S^{LW} \delta_L^{LW})^{1/2}+(\delta_S^{+} \delta_L^{-})^{1/2}+(\delta_S^{-} \delta_L^{+})^{1/2}) \quad (3)$$

X-ray photoelectron spectroscopy (XPS) measurements were performed on a K-Alpha spectrometer from ThermoFisher, equipped with a monochromated X-ray Source (Al Kα, 1486.6 eV). For all measurements a spot size of 400 µm was employed corresponding to an irradiated zone of ~ 1 mm^2. The hemispherical analyzer was operated in CAE (Constant Analyzer Energy) mode, with a pass energy of 200 eV, a step of 1 eV for the acquisition of surveys spectra, a pass energy of 50 eV and a step of 0.1 eV for the acquisition of narrow scan spectra. A “dual beam” flood gun was used to neutralize the charge build-up. The recorded spectra were processed by means of the Avantage software, using a peak-fitting routine with Shirley background and symmetrical 70%-30% mixed

Gaussian-Lorentzian line shapes. Atomic percentages were calculated following normalizations of peak areas using the Scofield sensitivity factors. During the fitting procedure, the components added to the core-level spectrum were constrained to have the same line shape and similar FWHM. The number of components was decided based on the molecule chemical structure and the knowledge of chemical shifts from databases and the literature. Additional constraints were added concerning the BE and the area ratio of different components. In order to check the quality of fit, normalized areas of corresponding components from all core-level spectra were compared and found to be in the limit of precision for XPS (5-15%).The binding energy scale was calibrated against neutral carbon considered at 285 eV. The precision in binding energy is ± 0.2 eV. Four different area at the sample surface were measured in order to check the homogeneity of the grafted layer.

Spectroscopic Ellipsometry (SE) measurements were made using a Jobin Yvon UVISEL2 setup at an incidence angle of 70° [28]. The spectra were recorded over a 1.5-6 eV range with 0.05 eV resolution. The refractive indices, as well as the thicknesses, were deduced from the experimental data by using a dispersion law in DeltaPsi2 software. The corresponding optical dispersion is single oscillator derived from the Forouhi-Bloomer model which is applicable to dielectrics material [29].

The topography and the roughness of the films have been investigated by a Pico SPM-LE AFM from Molecular Imaging in tapping mode.

2.3. Synthesis of photoinitiator

Synthesis of tetraethyl-aminomethylene-bisphosphonate (1). Under argon, phosphorus oxychloride (3.38 g, 2.04 mmol, 1.9 eq) was slowly added (1 hour) to a mixture cooled at -10 °C containing formamide (0.48g, 1.07 mmol, 1 eq) and triethylphosphite (3.29 g, 2.14 mmol, 2eq). The reaction mixture was stirred at room temperature for 1 hour and then poured over a mixture of ice and ammonium hydroxide (40 ml). The aqueous layer was extracted with CH_2Cl_2 (3 x 50 ml) and the combined organic layers were evaporated under reduced pressure. The crude oil was dissolved in CH_2Cl_2 and treated with 5 % aqueous solution of hydrochloric acid until pH = 1. The aqueous layer was washed with CH_2Cl_2 (3 x 50 ml) and basified with a 2M NaOH solution until pH = 10. The aqueous layer was extracted with CH_2Cl_2 (4 x 50 ml) and the combined organic layers were dried over anhydrous $MgSO_4$, filtered and concentrated under reduced pressure. The product was obtained as colorless liquid (960 mg, Yield = 30 %).

NMR ^{1}H (500 MHz, $CDCl_3$) δ 4.23-4.09 (m, 8H), 3.44 (t, 1H, $^2J_{PH}$ = 20.4 Hz), 1.88 (bs, 2H,), 1.36 (t, 12H, $^3J_{HH}$ = 7.0 Hz). NMR ^{13}C (126 MHz, $CDCl_3$) δ 63.1 (m), 47.62 (t, $^1J_{CP}$ = 144.5 Hz), 16.3. NMR ^{31}P (202 MHz, $CDCl_3$) δ 20.2.

Synthesis of tetraethyl- (4-dimethylamino)benzamido)methylenebisphophonate (2). To a stirred solution of tetraethyl-aminomethylenebisphosphonate (0.74 g, 2.4 mmol, 1 eq) in dry THF were added triethylamine (0.60 g, 0.84 ml, 6 mmol, 2.5 eq) and then 4-dimethylaminobenzoylchloride (0.49 g, 2.7 mmol, 1.1 eq) at 0 °C. The solution was allowed to warm to room temperature and stirred under argon for 24 hours. The reaction mixture was diluted with water (10 ml) and extracted with CH_2Cl_2 (3 x 30 ml). The combined organic layers were dried over anhydrous $MgSO_4$ and evaporated under reduced pressure. The crude product was purified by silica gel column chromatography with AcOEt /MeOH (95:5). The pure product was obtained as a white powder (950 mg, Yield = 88 %).

m.p = 113 °C. NMR ^{1}H (500 MHz, $CDCl_3$) δ 7.72 (d, 2H, $^3J_{HH}$ = 8.9 Hz), 6.68 (d, 2H, $^3J_{HH}$ = 8.9 Hz), 6.56 (d, 1H, $^3J_{HH}$ =10.1 Hz), 5.31 (td, $^3J_{HP}$ = 21.6 Hz, $^3J_{HH}$ = 10.1 Hz, 1H), 4.21 (m, 8H), 3.03 (s, 6H), 1.26 (t, 6H, $^3J_{HH}$ = 7.0 Hz), 1.23 (t, 6H, $^3J_{HH}$ = 7.1 Hz). NMR ^{13}C (126 MHz, $CDCl_3$) δ 166.1, 152.8, 128.7, 119.6, 111.0, 63.6 (m), 43.6 (t, $^1J_{CP}$ = 147.3 Hz), 40.1, 16.4 (t, $^3J_{CP}$ = 2.9 Hz), 16.3 (t, $^3J_{CP}$ = 3.1 Hz). NMR ^{31}P (202 MHz, $CDCl_3$): δ(ppm) 16.8.

HRMS m/z (ESI): calcd. for $C_{18}H_{33}N_2O_7P_2$ $[M+H]^+$:451.1763, found: 451.1766.

Synthesis of 4-(dimethylamino)benzamido)methylene)bis(phosphonic acid (3). To a stirred solution of compound **2** (0.1g, 0.22 mmol, 1 eq) dissolved in dry CH_2Cl_2 (3 ml) was added bromotrimethylsilane (0.20 g, 1.32 mmol, 6 eq) under an argon atmosphere at 0 °C. The resulting mixture was stirred for 24 hours at room temperature. After evaporation of volatile compounds under reduced pressure, EtOH (2 ml) and H_2O (1ml) were added to give a white precipitate. The mixture was stirred at room temperature for 1 h. After filtration, bisphosphonic acid **3** was obtained as a white solid (70 mg, Yield = 94 %).

NMR ^{1}H (500 MHz, D_2O + NaOD) δ 7.42 (d, 2H, $^3J_{HH}$ = 8.7 Hz), 6.54 (d, 2H, $^3J_{HH}$ = 8.7 Hz), 3.88 (t, 1H, $^2J_{HP}$ = 18.7 Hz), 1.31 (s, 6H). NMR ^{13}C (126 MHz, D_2O + NaOD) δ 167.7, 152.8, 128.4, 121.4, 112.4, 50.38, 39.7. NMR ^{31}P (202 MHz, D_2O + NaOD) δ 14.7.

HRMS m/z (ESI): calcd. for $C_{10}H_{15}N_2O_7P_2$ $[M-H]^-$: 337.0354, found: 337.0362.

2.4. Preparation of Yttria Tetragonal Zirconia polycrystal (Y-TZP) disks

The Y-TZP samples were obtained from a Tosoh TZ-3YB-E zirconia ZrO_2 powder with 3 mol% Y_2O_3 (particle size 40 nm). A quantity of 1.5 g of the powder (1.15 x 10^{-2} mol of ZrO_2 and 5.56 x 10^{-4} mol of Y_2O_3) was introduced into a 1.6 cm diameter mold and pressed at 100 MPa. The Y-TZP disks were placed in the oven and sintered at 1500 ◦C for 2 hours under static air. The heating and cooling ramps were 150 ◦C/h. After cooling to room temperature, we obtained yttria zirconia disks (diameter: 13 mm, thickness: 3 mm). Then, Y-TZP disks were polished mechanically with abrasive papers (220-grit, 500-grit and 1200-grit) and water. Then, they were polished with Largo, DAC and NAP abrasives

papers and diamond solutions down to 1 µm to obtain Y-TZP disks. Finally, the Y-TZP were ultrasonically cleaned in acetone and then dried for a few minutes under argon atmosphere. Before grafting, the Y-TZP disks were cleaned and activated by freshly prepared "piranha" (98 % H_2SO_4/30 % wt H_2O_2 in H_2O; 70/30 v/v) for 1 hour at room temperature and rinsed thoroughly with deionized water until neutral pH (Y-TZP-OH surfaces).

2.5. Grafting of initiator acid on Y-TZP-OH surface

In a sealed tube, the synthesized initiator compound **3** (2 mg) was dissolved in 4 ml of ultrapure water (Milli-Q®) by adding a few drops of NaOH solution (1M) up to pH = 9-10. Piranha treated zirconia (Y-TZP-OH) samples were dipped in the solution and heated to 100 °C for 4 hours without stirring. At the end of the reaction, the grafted surfaces (Y-TZP-O-P) were thoroughly washed with ultrapure water in order to remove unreacted bisphosphonic acid (three times for 5 minutes) and then dried under argon atmosphere.

2.6. General procedure for visible light induced conventional radical polymerization

In a screw vial clear glass, monomer (4 ml, styrene or methyl methacrylate), camphorquinone (31 mg) and the zirconia pellet grafted with initiator were degassed with argon for 20 minutes. The mixture was irradiated using a blue light lamp (450 - 455 nm) at room temperature for 2 hours. The resulting Y-TZP surfaces (Y-TZP-PS or Y-TZP-PMMA) were washed several times in CH_2Cl_2 and THF then by acetone, dried under argon and then under vacuum for a few hours.

3. Results and discussion

The functionalization of Y-TZP surface with polymers by adopting the "grafting from" method was accomplished in a three-steps process as outlined in Scheme 1. In the *Step A*, a zirconia pellet was prepared from the molecular precursors followed by several treatments to activate its surface. In the *Step B*, the Y-TZP-OH surface was reacted with amido methylenebisphosphonic acid to graft the photopolymerization initiator group (Y-TZP-O-P surface). The last step (*step C*) involved the surface-initiated photopolymerization of methyl methacrylate or styrene monomers by light irradiation (Y-TZP-PS or Y-TZP-PMMA surfaces).

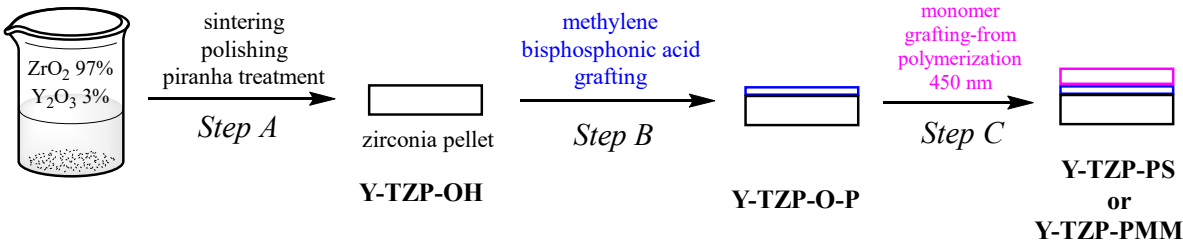

Scheme 1. Schematic representation of zirconia surface modification using bisphosphonic acid as anchoring agent.

3.1 Synthesis of amido bisphosphonic acid as anchoring agent and its surface grafting

In order to carry out the "grafting-from" photopolymerization on the zirconium oxide surfaces, the design of a molecule bearing two functional groups, namely an anchoring function and a second function allowing the initiation of the radical photopolymerization is fundamental.

The commonly used initiating system for the radical photopolymerization process (for example for dental composites) is the system based on camphorquinone with a tertiary amine. Indeed, the Norrish type II reaction generate radicals by direct hydrogen abstraction using a coinitiator (hindered tertiary amine) in order to allow an effective polymerization [30-32]. In our study, the 4-dimethylaminophenyl group was selected as an initiator according to recent results published in our group [33].

In summary, the grafting agent combines a 4-dimethylaminophenyl group with a bisphosphonic acid derivative linked by a covalent bond using an amide function. The chemical structure of this molecule is presented in Figure 1. Its synthesis was carried out in three steps as shown in Scheme 2.

Figure 1. Chemical structure of grafting and photoinitiator agent

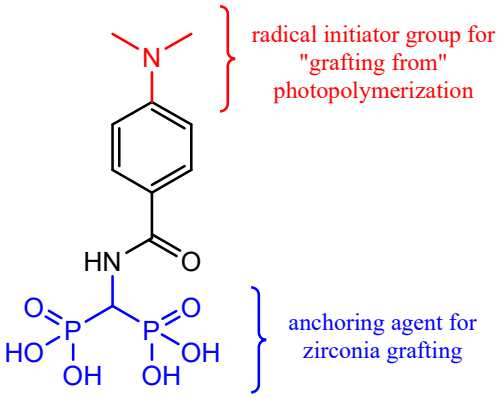

Firstly, methylene amino bisphosphonate **1** was synthesized in a one-pot procedure involving a Vilsmeir-Haack type intermediate (combination of formamide with $POCl_3$) followed by a nucleophilic attack of triethylphosphite according to a Michaelis-Arbuzov type reaction [34]. In this sequence, compound **1** was obtained in 30 % yield from the readily available commercial reagents. NMR

analyzes have confirmed the purity of the product which can be used without purification. Subsequently, the previous amine reacted with 4-(dimethylamino)benzoyl chloride to give methylene amido bisphosphonate **2** in 88 % yield**.** The methylene amidobisphosphonic acid **3** was prepared by dealkylation of the phosphonate groups, upon treatment with excess of trimethylsilyl bromide followed by ethanolysis (Scheme 2). The ^{1}H and ^{31}P NMR spectra of molecules 1, 2 and 3 were in good agreement with the expected chemical structures (Figure 2).

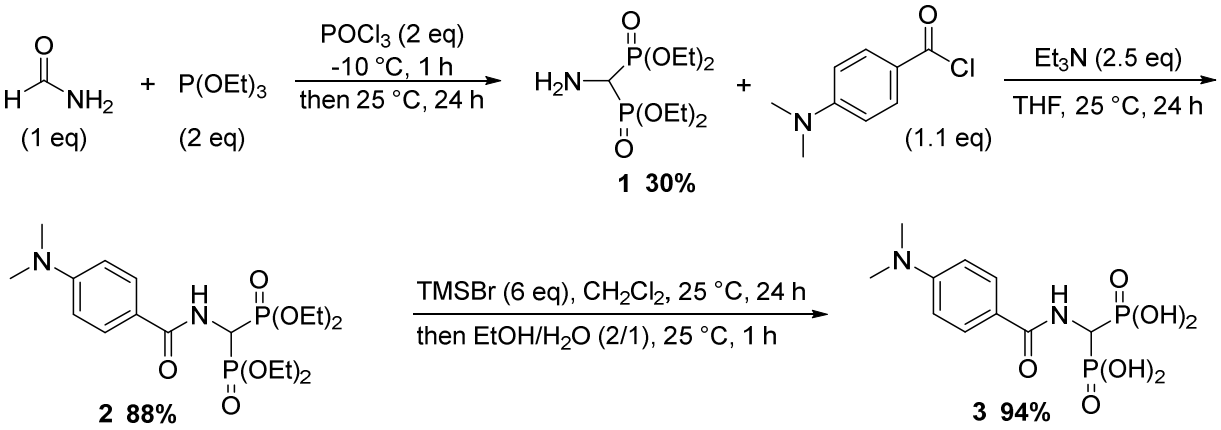

Scheme 2. Synthesis of the amido bisphosphonic photoinitiator **3**

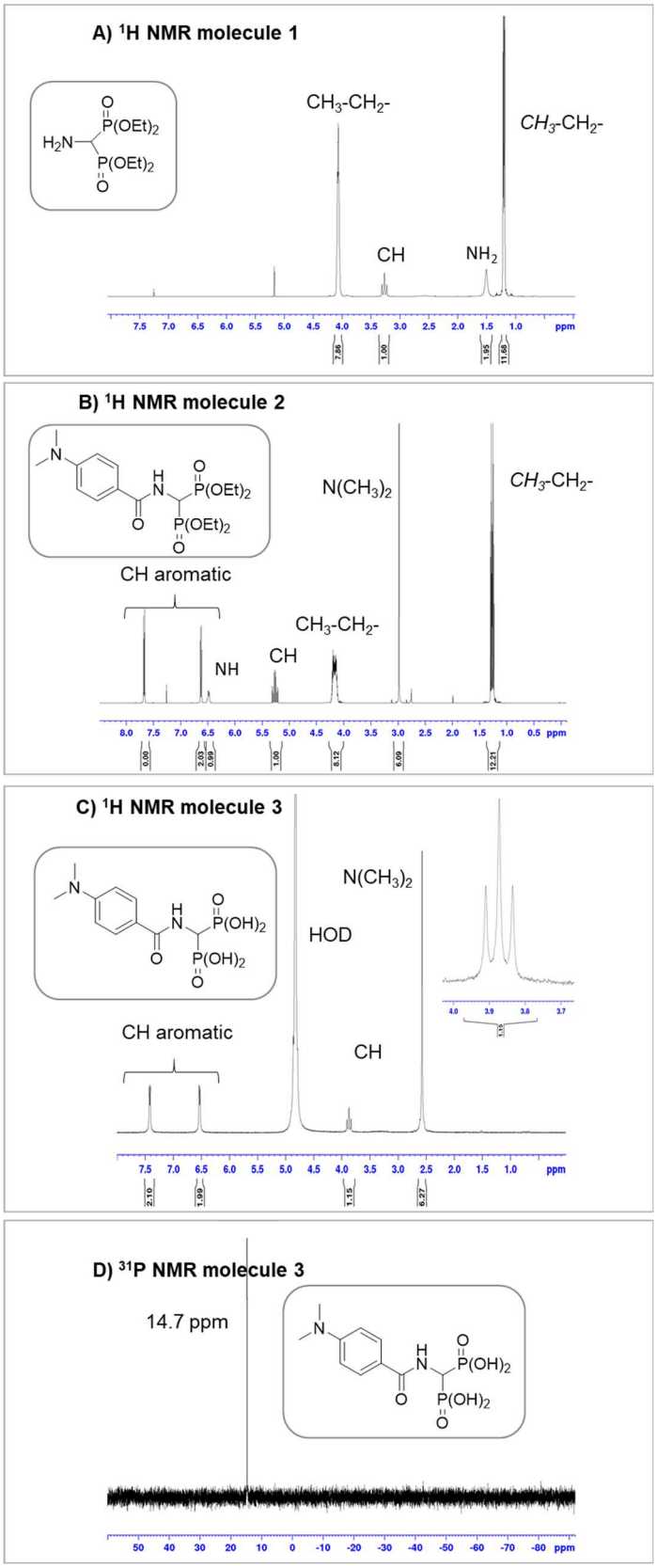

Figure 2. ^{1}H NMR spectra (A, B and C) of molecules **1**, **2** and **3**, respectively and ^{31}P NMR spectrum (D) of molecule **3** (solvent: $CDCl_3$ for molecules **1** and **2**, D_2O for molecule **3**)

The procedure of the Y-TZP surfaces preparation is depicted in Figure 3. The ceramics were successfully obtained using a Tosoh TZ-3YB-E powder (97 mol% ZrO_2 stabilized by 3 mol% Y_2O_3). The Y-TZP disks were pressed and sintered at 1500 °C for 2 hours followed by polishing. Then, they were treated with a piranha solution according to our previously reported procedure [33]. This treatment removes all the organic residues coming from the polishing step [35,36]. It also allows the oxidation of the surface by introducing hydroxyl groups (Y-TZP-OH) which increase the surface hydrophilicity and wettability. The surface topography evaluated by tapping mode AFM gives a Root Mean Square (RMS) roughness equal to 1.4 nm (Figure 3).

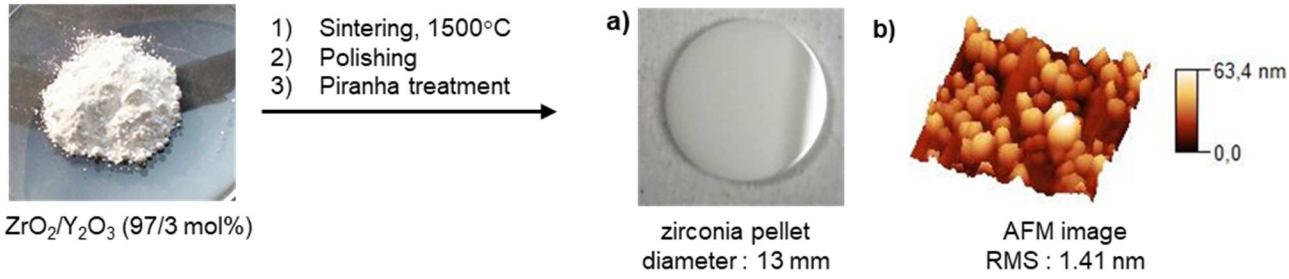

Figure 3. Photo of Y-TZP surface after polishing **(a)** and AFM topography image of Y-TZP surface (**b**).

To confirm the chemical functionalizations of Y-TZP, XPS analyses were performed at each grafting step of the process. This characterization technique allows knowing the atomic composition of zirconia surface. Table 2 exposes the estimated atomic percentages of each element determined by XPS. After treating with piranha solution, the atomic carbon concentration decreased to 8.6 % due to removal of organic contamination such as hydrocarbons. Conversely**,** atomic concentration of zirconium and oxygen increased to 29.9 % and 59.7 % respectively, which is consistent with the theoretical values of zirconium oxide (ZrO_2).

The evolution of the surface state after each step can be followed by water contact angle measurements. This simple and fast measurement allows validation of the modifications made on the surfaces during the grafting steps. The water contact angle of the native Y-TZP is close to 60° (due to the presence of organic residues) which is consistent with literature data [27]. After the piranha treatment, the water contact angle value decreases to 21° (Y-TZP-OH) due to the elimination of organic contamination and the formation of hydroxyl groups.

Table 2. Atomic percentages of species on zirconia surface obtained from XPS analysis after the different surface treatments.

	Experimental atomic ratio %					
Surfaces	**C1s**	**O1s**	**Zr3d**	**Y3d**	**P2p**	**N1s**
Y-TZP	19.5	54.6	24.4	1.5	-	-
Y-TZP-OH	8.6	59.7	29.9	1.8	-	-
Y-TZP-O-P	13.4	58.0	26.6	1.4	0.6	0.5
Y-TZP- PS	94.9	3.9	1.2	-	-	-
Y-TZP- PMMA	73.5	26.4	0.1	-	-	-

We tested the reactivity of the Y-TZP surface with bisphosphonic acid **3** in different conditions. To promote the condensation of hydroxyl groups of Y-TZP-OH, we studied the influence of concentration, pH, temperature and reaction time then the grafting was evaluated by ellipsometry. As shown in Table 3, the best results were obtained under basic conditions (pH = 9) with a concentration of 1.5 mmol L^{-1} in bisphosphonic acid and heating the mixture at 100 °C for 4 hours. Indeed, a basic pH is necessary to obtain good solubility of compound **3** in water at 100 °C. The thickness of the initiator determined by ellipsometry increases over time (for example 9 and 20 nm for 12 and 24 hours reaction time, respectively), possibly by the tendency of phosphonic acid groups to condensate to dimers, trimers or higher polycondensates as was previously observed [37]. A proposition of structure is given on Figure 4.

Table 3. Grafting of amido bisphosphonic acid initiator onto Y-TZP-OH surface (experimental conditions and thickness determined by ellipsometry)

Entry	**[initiator 3] mmol.L^{-1}**	**time**	**temperature (°C)**	**thickness (ellipsometry) (nm)**
1	15	4h	100	1.4
2	1,5	4h	100	2.6
3	1.5 (pH=9)	24h	25	0.8
4	1.5 (pH =9)	4h	100	3.3
5	1.5 (pH =9)	12h	100	9
6	1.5 (pH=9)	24h	100	20

The chemical composition of the surface (determined by XPS) after bisphosphonic acid grafting is reported in Table 2 (Y-TZP-O-P). A decrease of the Zr and Y element signals was observed, confirming the presence of an organic layer. Two new peaks appeared corresponding to N1s and P2p with atomic percentages equal to 0.5 and 0.6, respectively. The N1s peak around 400 eV was assigned to the amide (400.2 eV) and amine functions (399.2 eV) (Figure 5 (A)). The C1s region was fitted with four peaks (285.1, 286.5, 288.7 and 293.4 eV) assigned to C-C/C=C/C-H, C-N, C=O species and to the shake-up of π electrons, respectively (Figure 5 (C)). In addition, a significant increase of carbon species was observed (from 8.6 % before grafting to 13.4 % before grafting). The P2p core-level spectrum (Figure 5 (B)) showed the spin-orbit coupling doublet, its components are located at 134.0 eV (P 2p½) and 133.1 eV (P 2p3/2) with the expected separation of 0.9 eV and the 0.5 area ratio. According to this results (observation of a single peaks series for P2p) and by comparison with other published results, we assumed that phosphonic acid adsorbs in a bidentate geometry following deprotonation of phosphonate hydroxyl groups and leaving the P=O group unbound (PO_3^{2-} species), a representation is proposed on Figure 4 [38]. In a recent publication related to the grafting of bisphonic acid on zirconia nanoparticles, the formation of bidentate anchoring by reaction of P-OH to form P-O-Zr was characterized by solid state ^{31}P NMR. The same study provided additional information coming from ^{1}H NMR MAS, no signal assigned to P-OH was observed [39]. However, the exact assignment of this component remains complicated by the proximity of the binding energies of the single ($PO_2(OH)^-$) and double (PO_3^{2-}) coordination mode [40].

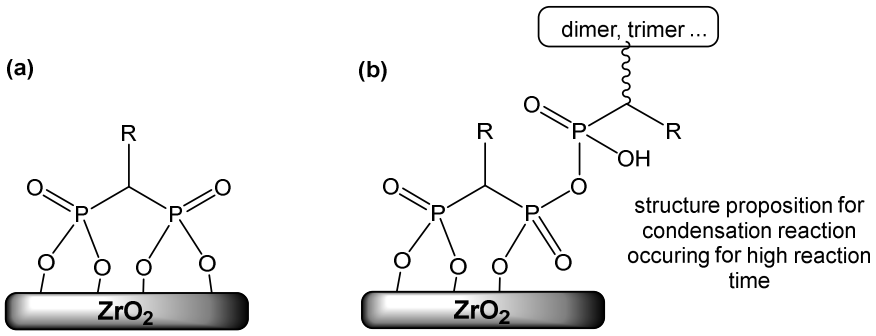

Figure 4. Functionalization of zirconia by amido bisphosphonic acid according a bidentate geometry (a) and the possible formation of dimers and trimers by condensation reaction for higher reaction time (b).

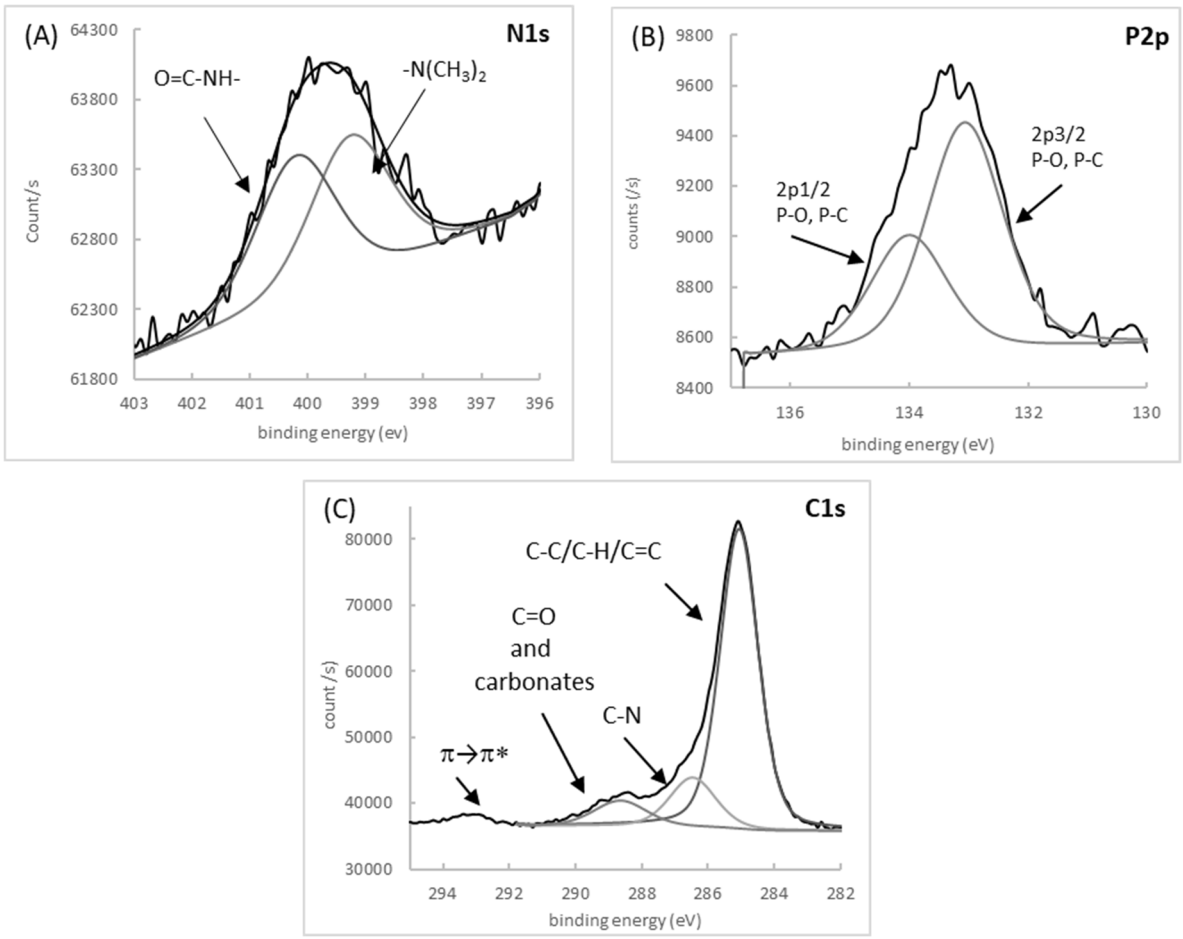

Figure 5. Core-level spectra of N1s (A), P2p (B), and C1s (C) after initiator grafting

In order to confirm the grafting of the initiator on the surface, water contact angle measurements were carried out. After reaction, the water contact angle value increased from 21° to 56.7 ° indicating a reduction in hydrophilicity by covering the zirconia surface with an amido-bisphosphonic acid layer. This result is in agreement with chemical structure of the grafted molecule. In literature, a similar result was obtained after the grafting of a phosphonic acid bearing an alkyl chain [41].

3.2. Grafting- from photo-polymerization of model monomers

Once steps A and B were successful, we studied the photopolymerization reaction with camphorquinone as a widely used photoinitiator in dentals applications. The bulk photopolymerization of the two model monomers (MMA and styrene) was carried out under light irradiation (Scheme 1).

Actually, many publications have investigated the mechanism of camphorquinone – amine photoinitiating system [25,31,42]. Camphorquinone absorbs radiation in the region of 200-300 nm

(π,π* transition) and in visible light 400-500 nm (responsible for its yellow color) due to the n,π* transition of the α-dicarbonyl chromophore. Absorption of light by camphorquinone leads to the formation to excited states: the "singlet state" and the "triplet state" which is the one relevant to free radical formation and which have a very short half-life. While the "triplet state", the camphorquinone molecule can interact with the amine group grafted on the surface to generate an excited state complex ("exciplex") [31]. In this state, the camphorquinone molecule abstracts a hydrogen atom from the tertiary amine on the surface resulting in the formation of free radicals. Then, photoinitiated polymerization occurs by a chain reaction between the free radicals formed on the surface and the monomer (styrene or MMA). A proposition of mechanism is presented on Scheme 3.

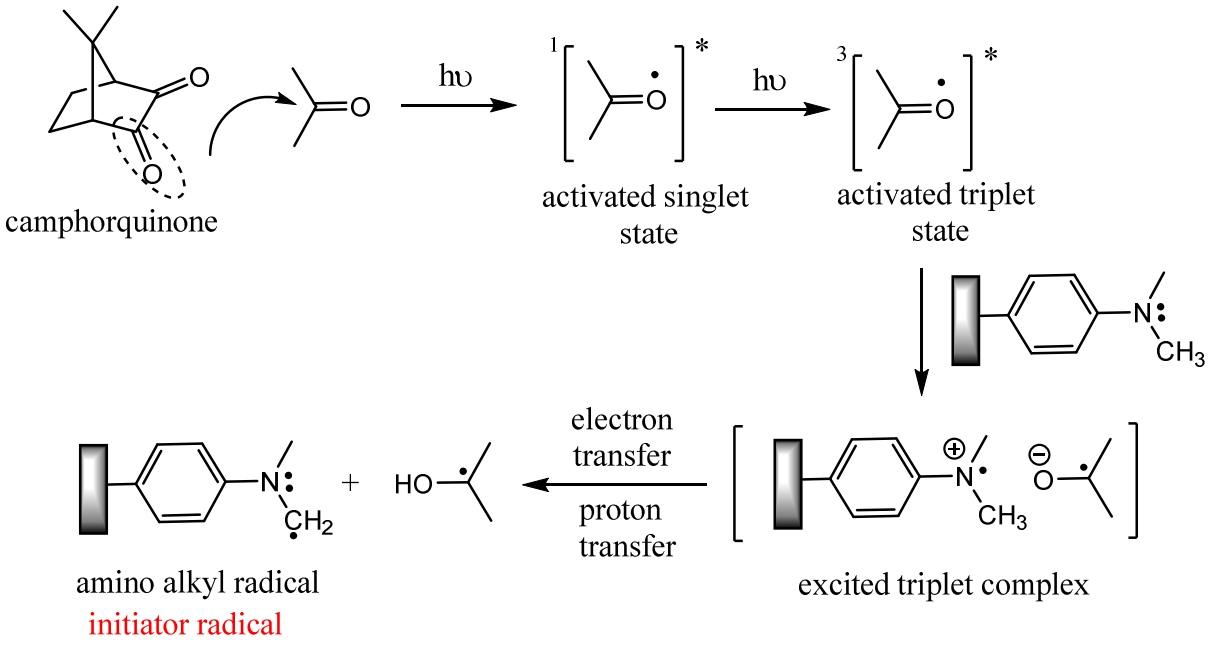

Scheme 3. Possible reaction mechanism of photoinitiator system with camphorquinone and amine [42]

MMA or styrene photopolymerization was performed by irradiation with a blue light lamp (450 - 455 nm) at room temperature for 2 hours, followed by a careful rinsing of the zirconia surfaces with polymer good solvents (THF and CH_2Cl_2). Once again, contact angle measurements were performed to control this step. After MMA polymerization (Y-TZP-PMMA surface), the water contact angle increased from 56 ° to 73 ° whereas the surface became more hydrophobic with a contact angle equal to 85 ° after styrene polymerization (Y-TZP-PS). The contact angle evolution after each step are presented on Figure 6. The water contact angle values obtained for Y-TZP-PMMA and Y-TZP-PS

surfaces were in good agreement with values reported in literature for grafted or neat polystyrene or PMMA surfaces [12, 43-45].

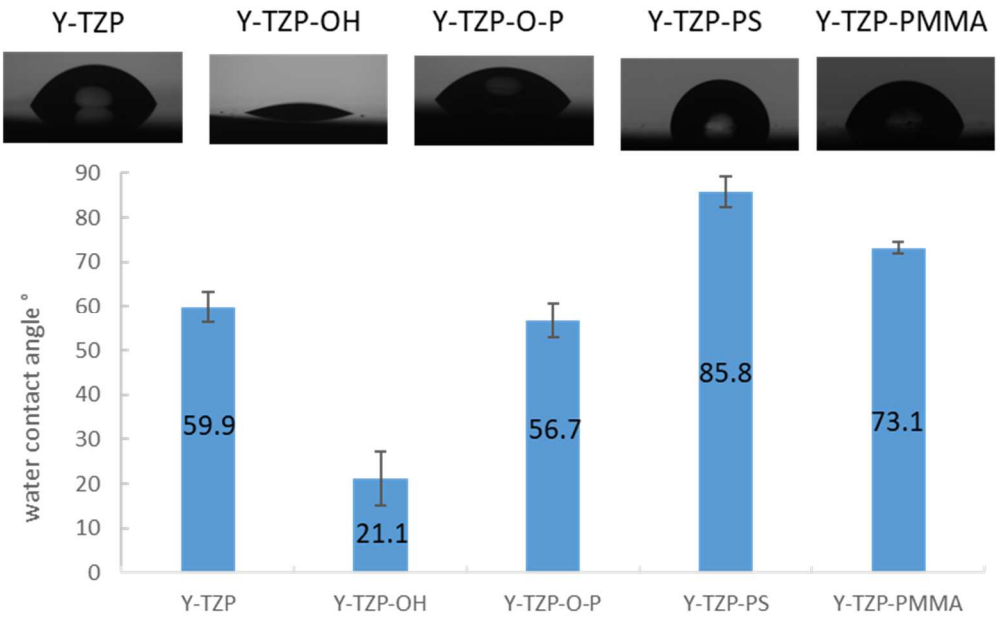

Figure 6. Evolution of water contact angle after the different chemical treatments (piranha treatment, photoinitiator grafting and photopolymerizations).

After styrene (monomer unit C_8H_8) polymerization, the atomic percentage of carbon determined by XPS increased from 13.4 (after initiator grafting) to 94.9 (Table 2, step C). At the same time, a significant attenuation of oxygenated species signal was observed (from 58.0 % before polymerization to 3.9 % after polymerization). The C1s core-level spectrum is shown in Figure 7 (A) with a main C1s peak at 284.5 eV due to C-C/C-H bonds. The components related to carbon bonded to O, P and N have disappeared. In addition, a π-π* shake-up satellite peak at 291.1 eV due to the PS phenyl ring was observed [33].

The topographies of the zirconia surfaces after styrene polymerization investigated by AFM technique are shown in Figure 7 (B). The Root Mean Square (RMS) is equal to 23 and 29 nm for 1 µm and 2.5 µm size, respectively. Compared to surface after initiator grafting, a small increase of surface roughness was observed.

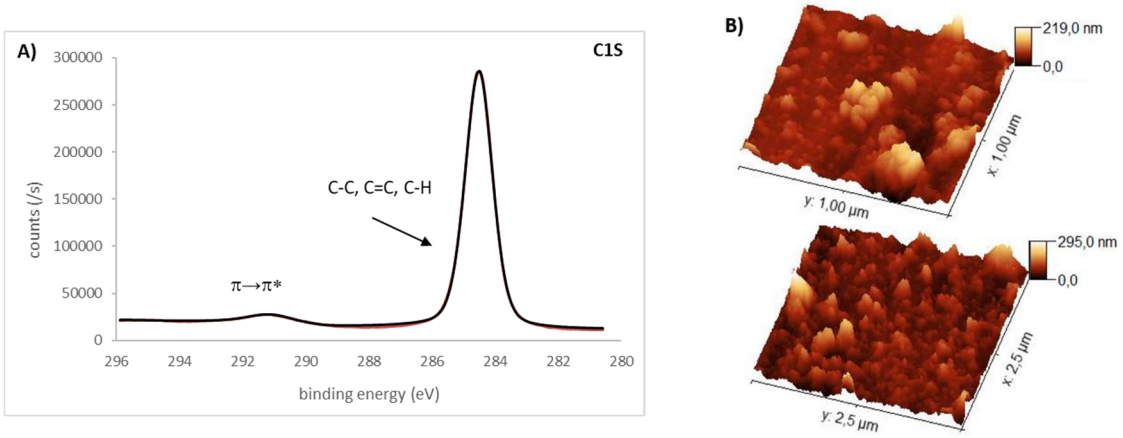

Figure 7. Core-level spectrum of carbon C1s (A) after styrene polymerization (step C) and AFM height image 3D of zirconia surface after styrene polymerization (B)

Also, after MMA polymerization (monomer unit $C_5H_8O_2$), the atomic percentage of carbon increased while a decrease of oxygenated species was observed. The values are presented in Table 2 (step D, Y-TZP-PMMA). The C1s core-level spectrum peak after MMA polymerization changes significantly and can be fitted with four carbon components (Figure 8 (A)): a main peak for C-C/C-H (284.9 eV, 46 %) and three less intense peaks for C*-COO (285.7 eV, 20 %), C–O (286.8 eV, 18 %) and C=O (288.9 eV, 16 %). The O1s signal was fitted with two components coming from oxygenated species of monomer and corresponding to C=O (532.2 eV) and C-O (533.8 eV) (Figure 8 (B)).

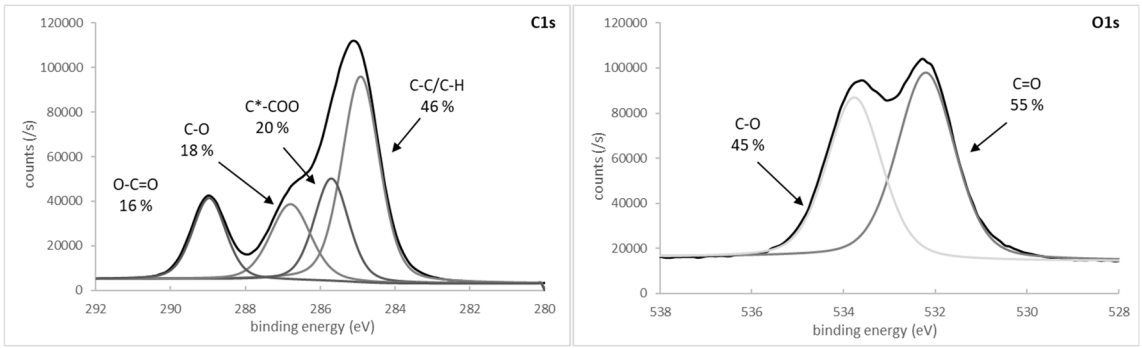

Figure 8. Core-level spectra of carbon C1s (A) and O1s (B) after MMA polymerization

The RMS of the PMMA is equal to 6 and 9 nm for 1 µm and 2.5 µm size, respectively. As previously observed for PS grafting, a slight increase of surface roughness is obtained after PMMA grafting. This phenomena can be explained by a non-uniformity in molar masses probably due the polymerization mechanism (irreversible termination reactions in conventional radical polymerization) (Figure 9).

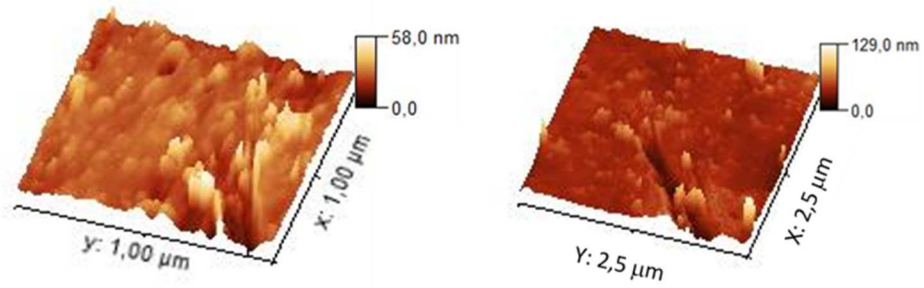

Figure 9. AFM height image 3D of zirconia surface MMA polymerization

In order to calculate the surface energies, the dispersive and the surface polarity of the materials, we supplemented the contact angle analyses by measurements on two other polar and non-polar liquids (formamide and diiodomethane). Results are presented on Figure 10.

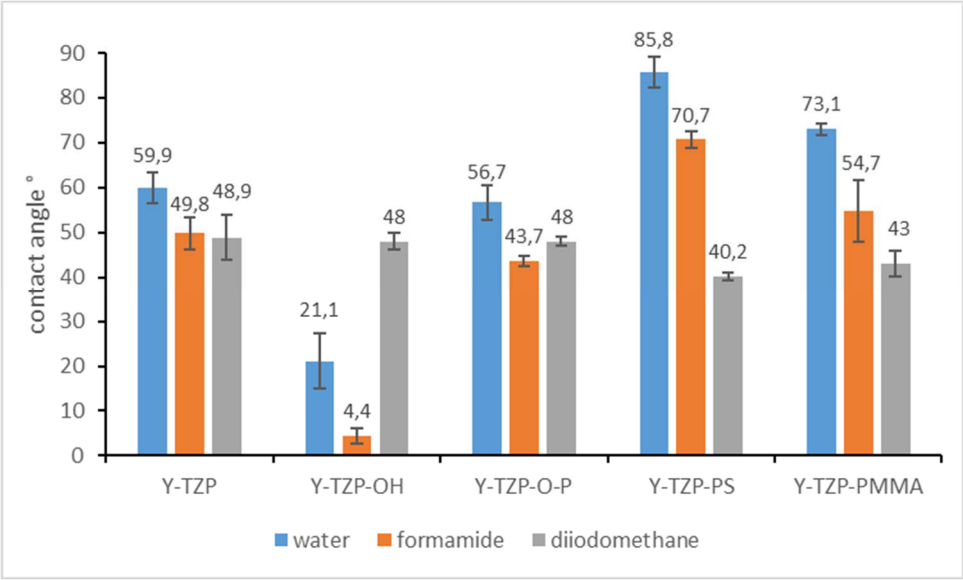

Figure 10. Contact angles measurements (water, formamide, diiodomethane) of native and modified Y-TZP surfaces**.**

From the Young-Van Oss equation, it was possible to calculate the Lifshitz-Van der-Waals δ^{LW} (nonpolar) and the Lewis acid-base contributions δ^{AB}. The δ^{AB} was calculated from the electron-donor δ^{s-} and electron-acceptor δ^{s+} parameters [26,27,46]. The values for all these parameters are summarized in Table 4.

Table 4. Calculated values of the surface energy δ_S, the component Lifshitz-Vand-Der-Waals δ^{LW}, the electron acceptor δ^+ and the electron donor δ^- parameters of the acid-base component of native and modified Y-TZP surfaces.

Surface	Surface energetic characteristics (mJ.m^{-2})			
	δ_s	δ^+	δ^-	δ^{LW}
Y-TZP	40.32	0.32	23.05	34.89
Y-TZP-OH	57.87	2.56	45.86	36.2
Y-TZP-O-P	43.83	0.78	22.88	35.4
Y-TZP-PS	35.50	0.56	7.11	31.5
Y-TZP-PMMA	40.46	0.14	10.43	38.0

The total surface energy (δ_S) of native Y-TZP is equal to 40.3 2 mJ.m^{-2}, in reasonable agreement with others studies [27]. The polar components (δ^+ and δ^-) were relatively low, these values corroborating the presence of organic impurities. After piranha treatment, total surface energy (δ_S) increased to 57.8 mJ.m^{-2} and the electron donor δ^- component increased to 45.82 mJ.m^{-2} due to the presence of numerous hydroxyl groups (Y-TZP-OH) on the surface. Reaction with amido bisphosphonic acid led to a decrease of the electron donor δ^- component (22.8 .2 mJ.m^{-2}) due to the formation of Y-TZP-O-P bonds. Then, styrene and MMA photopolymerizations giving more hydrophobic surface led to a decrease in the total surface energy (35.5 and 40.4 mJ.m^{-2} respectively) as well as the electron donor δ^- component.

The thickness of the PMMA and PS polymer grafting was determined by SE. The thickness of the organic layer formed from grafted initiator was found to be around 3.4 nm. After photopolymerization with MMA and styrene, the thickness increased to 27.3 and 45.5 nm, respectively. These results are reported in Table 5.

These different characterizations confirmed the photopolymerization efficiency and the formation of grafted polymer layer on the zirconia surface. By this method, we will be consider extending this zirconia surface functionalization to several monomers including zwitterionic compounds and ionic liquids in order to propose new antibacterial or antiobioadhesive surfaces.

Table 5. Evolution of the surface thickness determined by spectroscopic ellipsometry after different modification step

Surface	**Thickness (nm)**
Photoinitiator grafting (Y-TZP-O-H)	3.3
Styrene polymerization (Y-TZP-PS)	27.3
MMA polymerization (Y-TZP-PMMA)	45.4

4. Conclusion

In this study, we reported a simple strategy to modify the zirconia surfaces by grafting-from photopolymerization. To this end, a new photoinitiator bearing a *N*,*N*-dimethylamine function and a bisphosphonic acid was designed. Effective grafting of this organic initiator on the zirconia surface has been successfully achieved by condensation of its phosphonic acid functions with the surface hydroxyl groups.

Subsequently, we evaluated the "grafting from" photopolymerization reactions with styrene or methyl methacrylate as monomers by blue light activation. After grafting and polymerizations of these monomers, the surface modifications were characterized by AFM, XPS and SE. The XPS study showed clearly all characteristic peaks corresponding to the atoms and functional groups coming from the photoinitiator and grafted polymers. The wettability of the surface was characterized by measurements of contact angles at different polar and nonpolar liquids to calculate the energy of surfaces and its polar parameters.

Author contributions

The manuscript was written through the contributions of all authors. All authors have approved the final version of the manuscript.

Declaration of Competing Interest

The authors declare that they have no known competing financial interests or personal relationships that could have appeared to influence the work reported in this paper.

Data availability

No data was used for the research described in this article.

Acknowledgements

The authors thank “Région Normandie”, the European FEDER Normandie and the French Agence Nationale de la Recherche (ANR) in the framework of the SUZI project (RIN Recherche 2020 – Projet Emergent) for their financial support. The authors are grateful to Ministère de l’Enseignement Supérieur et de la Recherche Scientifique Tunisien (Université de Carthage) for providing a grant to Jihen Ben-Hadj-Salem.

References

[1] G. Soo, B. Pingguan-Murphy, K.W. Lai, S.A. Akbar, Review of zirconia-basel bioceramic: Surface modification and cellular response, Ceram. Int. 42 (2016) 12543-12555. https://doi.org/10.1016/j.ceramint.2016.05.077.

[2] M. Liu, J. Zhou, Y. Yang, M. Zheng, J. Yang, J. Tan, Surface modification of zirconia with polydopamine to enhance fibroblast response and decrease bacterial activity in vitro: A potential technique for soft tissue engineering applications, Colloids Surf. B Biointerfaces 136 (2015) 74-83. https://doi.org/10.1016/j.colsurfb.2015.06.047.

[3] T. Otsuka, Y. Chujo, Poly(methyl methacrylate) (PMMA)-based hybrid materials with reactive zirconium oxide nanocrystals, Polym. J. 42 (2010) 58-65. https://doi.org/10.1038/pj.2009.309.

[4] D. Li, J. Yao, B. Liu, H. Sun, S. van Agtmaal, C. Feng, Preparation and characterization of surface grafting polymer of ZrO_2 membrane and ZrO_2 powder, Appl. Surf. Sci. 471 (2019) 394-402. https://doi.org/10.1016/j.apsusc.2018.12.009.

[5] F.H. Schünemann, M.E. Galarraga-Vinueza, R. Magini, M. Fredel, F. Silva, J.C.M. Souza, Y. Zhang, B. Henriques, Zirconia surface modifications for implant dentistry, Mater.Sci. Eng C 98 (2019) 1294-1305. https://doi.org/10.1016/j.msec.2019.01.062.

[6] C. Caravaca, L. Shi, P. Rivory, E. Laurenceau, Y. Chevolot, D. Hartmann, L. Gremillard, J. Chevalier, Direct silanization of zirconia for increased biointegration, Acta Biomater. 46 (2016) 323-335. https://doi.org/10.1016/j.actbio.2016.09.034.

[7] M. Roy, A. Pompella, J. Kubacki, A. Poisik, B. Psiuk, J. Klimontko, J. Szade, R.A. Roy, W. Hedzelek, Photofunctionalization of dental zirconia oxide: Surface modification to improve bio-integration

preserving crystal stability, Colloids Surf B Biointerfaces 156 (2017) 194-202. https://doi.org/10.1016/j.colsurfb.2017.05.031.

[8] A. Chandra, E. Bhuvanesh, P. Mandal, S. Chattopadhyay, Surface modification of anion exchange membrane using layer-by-layer polyelectrolytes deposition facilitating monovalent organic acid transport, Colloids Surf A Physicochem. Eng. Asp. 558 (2018), 579-590. https://doi.org/10.1016/j.colsurfa.2018.09.013.

[9] S. Wang, Z. Wang, J. Li, W. Hu, Surface-grafting polymers: from chemistry to organic electronics, Mater. Chem. Front. 4 (2020) 692-714. https://doi.org/10.1039/C9QM00450E.

[10] R. Quinones, E.S. Gawalt, Polystyrene formation on monolayer-modified nitinol effectively controls corrosion, Langmuir 24 (2008) 10858-10864. https://doi.org/10.1021/la801906e.

[11] K. Woonjung, J. Jung, Polymer brush: a promising grafting approach to scaffolds for tissue engineering, BMB reports, 49 (2016) 655–661. https://doi.org/10.5483/bmbrep.2016.49.12.166.

[12] L. Bech, T. Elzein, T. Meylheuc, A. Ponche, M. Brogly, B. Lepoittevin, P. Roger, Atom transfer radical polymerization of styrene from different poly(ethylene terephthalate) surfaces: Films, fibers and fabrics, Eur. Pol. J. 45 (2009) 246-255. https://doi.org/10.1016/j.eurpolymj.2008.10.031.

[13] S. Akbarn, E. Beyou, P. Chaumont, J. Mazzolini, E. Espinosa, F. D'agosto, C. Boisson, Synthesis of polyethylene-grafted multiwalled carbon nanotubes via a peroxide-initiating radical coupling reaction and by using well-defined TEMPO and thiol end-functionalized polyethylenes, J Polym Sci Part A: Polym Chem, 49 (2011) 957-965. https://doi.org/10.1002/pola.24508.

[14] S.P. Pujari, L Scheres, A. T.M. Marcelis, H. Zuilhof, Covalent surface modification of oxide surfaces, Angew. Chem. Int. Ed. 53 (2014) 6322-6356. https://doi.org/10.1002/anie.201306709.

[15] R. Boissezon, J. Muller, V. Beaugeard, S. Monge, J.J. Robin, Organophosphonates as anchoring agents onto metal oxide-based materials: synthesis and applications, RSC Adv. 4 (2014) 35690. https://doi.org/10.1039/C4RA05414H.

[16] W. Gao, L. Dickinson, F.G. Morin, L. Reven, Self-assembled monolayers of alkylphosphonic acids on metal oxides, Langmuir 12 (1996) 6429-6435. https://doi.org/10.1021/la9607621.

[17] G. Guerrero, P. H. Mutin, A. Vioux, Anchoring of phosphonate and phosphinate coupling molecules on titania particles, Chem. Mater. 13 (2001) 4367-4373. https://doi.org/10.1021/cm001253u.

[18] C. A. Traina, J. Schwartz, Surface modification of Y_2O_3 nanoparticles, Langmuir 23 (2007) 9158-9161. https://doi.org/10.1021/la701653v.

[19] T.J. Daou, J.M. Grenèche, G. Pourroy, S. Buathong, A. Derory, C. Ulhaq-Bouillet, B. Donnio, D. Guillon, S. Begin-Colin, Coupling Agent Effect on Magnetic Properties of Functionalized Magnetite-Based Nanoparticles, Chem. Mater. 20 (2008) 5869. https://doi.org/10.1021/cm801405n.

[20] T. Schulmeyer, S. A. Paniagua, P. A. Veneman, S. C. Jones, P. J. Hotchkiss, A. Mudalige, J. E. Pemberton, S. R. Marder, N. R. Armstrong, Modification of $BaTiO_3$ thin films: adjustment of the effective surface work function, J. Mater. Chem. 17 (2007) 4563-4570. https://doi.org/10.1039/B706949A.

[21] C. J. Lomoschitz, B. Feichtenschlager, N. Moszner, M. Puchberger, K. Müllern M. Abele, G. Kickelbick, Directing Alkyl Chain Ordering of Functional Phosphorus Coupling Agents on ZrO_2, Langmuir 27 (2011) 3534-3540. https://doi.org/10.1021/la104527b.

[22] F. Brodard-Severac, G. Guerrero, J. Maquet, P. Florian, C. Gervais, P. H. Mutin, High-Field ^{17}O MAS NMR Investigation of Phosphonic Acid Monolayers on Titania, Chem. Mater. 20 (2008) 5191-5196. https://doi.org/10.1021/cm8012683.

[23] C.S. Griffith, M. De Los Reyes, NI Scales, J.V. Hanna, V. Luca, Hybrid Inorganic-Organic Adsorbents Part 1: Synthesis and Characterization of Mesoporous Zirconium Titanate Frameworks Containing Coordinating Organic Functionalities, ACS Appl. Mater. Interfaces 2 (2010) 3436-3446. https://doi.org/10.1021/am100891u.

[24] J. Svehla, S. Pabisch, B. Feichtenschlager, D. Holzmann, H. Peterlik, G. Kickelbick, Polyester Preparation in the Presence of Pristine and Phosphonic-Acid-Modified Zirconia Nanopowders, Macromol. Mater. Eng. 297 (2012) 219-227. https://doi.org/10.1002/mame.201100191.

[25] F. Morlet-Savary, J. E. Klee, F. Pfefferkorn, J.-P. Fouassier, J. Lalevée, The Camphorquinone/Amine and Camphorquinone/Amine/Phosphine Oxide Derivative Photoinitiating Systems: Overview, Mechanistic Approach, and Role of the Excitation Light Source, Macromol. Chem. Phys. 216 (215), 2161-2170. https://doi.org/10.1002/macp.201500184

[26] C. J. van Oss, M. K. Chaudhury, R. J. Good, Interfacial Lifschitz-van der Waals and Polar Interactions in Macroscopic Systems, J. Chem. Rev. 88 (1988), 927-941.

[27] M.L. González-Martín, L. Labajos-Broncano, B. Janczuk, J.M. Bruque, Wettability and surface free energy of zirconia ceramics and their constituents, J. Mater. Sci. 34 (1999): 5923-5926. https://doi.org/10.1023/A:1004767914895.

[28] http://www.horiba.com/scientific/products/ellipsometers/software/.

[29] A.R. Forouhi, I. Bloomer, Optical dispersion relations for amorphous semiconductors and amorphous dielectrics, Phys. Rev. B. 34 (1986) 7018–7026. https://doi.org/10.1103/PhysRevB.34.7018.

[30] R.Z. Douaihy, I. Telegeiev, H. Nasrallah, O. Lebedev, P. Bazin, A. Vimont, J.F. Chailan, A. Fahs, M. El-Roz, Synthesis of silica-polymer core-shell hybrid materials with enhanced mechanical properties using a new bifunctional silane-based photoinitiator as coupling agent, Mater. Today Commun. 27 (2021) 102248. https://doi.org/10.1016/j.mtcomm.2021.102248.

[31] J. Jakubiak, X. Allonas, J.P. Fouassier, A. Sionkowska, E. Andrejewska, L.A. Linden, J.F. Rabek, Camphorquinone-amines photoinitiating systems for the initiation of free radical polymerization, Polymer 44 (2003) 5219-5226. https://doi.org/10.1016/S0032-3861(03)00568-8.

[32] P. Xiao, J. Lalevée, X. Allonas, J.P. Fouassier, C. Ley, M. El-Roz, S.Q. Shi, J. Nie, Photoinitiation mechanism of free radical photopolymerization in the presence of cyclic acetals and related compounds, J. Polym. Sci., Part A: Polym. Chem. 48 (2010) 5758-5766. https://doi.org/10.1002/pola.24383.

[33] C. Dezanet, D. Dragoe, P. Marie, N. Harfouche, S. Froissart, A. Fouchet, J. Rouden, J. Lecourt, C. Harnois, P. Thébault, J. Baudoux, B. Lepoittevin, Zirconia surface polymer grafting via dopamine-assisted co-deposition and radical photopolymerization, Prog. Org. Coat. 173 (2022) 107202. https://doi.org/10.1016/j.porgcoat.2022.107202.

[34] X. Cui, M. A. Green, P. J. Blower, D. Zhou, Y. Yan, W. Zhang, K. Djanashvili, D. Mathe, D. S. Veresg, K. Szigetig, $Al(OH)_3$ facilitated synthesis of water-soluble, magnetic, radiolabelled and fluorescent hydroxyapatite nanoparticles, Chem. Commun. 51 (2015) 9332-9335. https://doi.org/10.1039/C5CC02259B.

[35] F. Rupp, L.Scheideler, N. Olshanska, M. de Wild, M. Wieland, J. Geis-Gerstorfer, Enhancing surface free energy and hydrophilicity through chemical modification of microstructured titanium implant surfaces, J. Biomed. Mater. Res. A 76 (2006) 323-334. https://doi.org/10.1002/jbm.a.30518.

[36] A. Noro, M. Kaneko, I. Murat, M. Yoshinari, Influence of surface topography and surface physicochemistry on wettability of zirconia (tetragonal zirconia polycrystal), J Biomed Mater Res Part B 101B (2013) 355–363. https://doi.org/10.1002/jbm.b.32846.

[37] B. Heggen, S. Roy, F. Müller-Plathe, Ab Initio Calculations of the Condensation of Phosphonic Acid and Methylphosphonic Acid: Chemical Properties of Potential Electrolyte Materials for Fuel Cell Applications, J. Phys. Chem. C 112 (2008) 14209-14215. https://doi.org/10.1021/jp803589w.

[38] M. Wagstaffe, A.G. Thomas, M.J. Jackman, M. Torres-Molina, K.L. Syres, K. Handrup, An Experimental Investigation of the Adsorption of a Phosphonic Acid on the Anatase TiO_2(101) Surface, J. Phys. Chem. C 120 (2016) 1693-1700. https://doi.org/10.1021/acs.jpcc.5b11258.

[39] K. Hossain, L. Florean, A. Del Tedesco, E. Cattaruzza, M. Geppi, S. Borsacchi, P. Canton, A. Benedetti, P. Riello, A. Scarso, Modification of Amorphous Mesoporous Zirconia Nanoparticles with Bisphosphonic Acids: A Straightforward Approach for Tailoring the Surface Properties of the Nanoparticles, Chemistry 27 (2021) 17941-17951. https://doi.org/10.1002/chem.202103354.

[40] P. Canepa, G. Gonella, G. Pinto, V. Grachev, M. Canepa, O. Cavalleri, Anchoring of Aminophosphonates on Titanium Oxide for Biomolecular Coupling, J. Phys. Chem. C 123 (2019) 16843-16850. https://doi.org/10.1021/acs.jpcc.9b04077.

[41] H. Byrd, S. Whipps, J. K. Pike, J. Ma, S. E. Nagler, D. R. Talham, Role of the template layer in organizing self-assembled films: zirconium phosphonate monolayers and multilayers at a Langmuir-Blodgett template, J. Am. Chem. Soc. 116 (1994) 295-301. https://doi.org/10.1021/ja00080a034.

[42] E.A. Kamoun, A. Winkel, M. Eisenburger, H. Menzel, Carboxylated camphorquinone as visible-light photoinitiator for biomedical application: Synthesis, characterization, and application, Arabian Journal of Chemistry 9 (2016) 745-754. http://dx.doi.org/10.1016/j.arabjc.2014.03.008.

[43] G. Bac, T. Park, I.-H. Song, Surface Modification of Polymethylmethacrylate (PMMA) by Ultraviolet (UV) Irradiation and IPA Rinsing, Micromachines 13 (2022) 1952. https://doi.org/10.3390/mi13111952.

[44] Y. Li, J.Q. Pham, K.P. Jonston, P.F. Green, Contact Angle of Water on Polystyrene Thin Films: Effects of CO2 Environment and Film Thickness, Langmuir 23 (2007) 9785-9793. https://doi.org/10.1021/la0636311.

[45] Y. Ma, X. Cao, X. Feng, Y. Ma, H. Zou, Fabrication of super-hydrophobic film from PMMA with intrinsic water contact angle below 90°, Polymer 48 (2007) 7455-7460. https://doi.org/10.1016/j.polymer.2007.10.038.

[46] B. Lepoittevin, T. Elzein, D. Dragoe, A. Bejjani, F. Lemée, J. Levillain, P. Bazin, P. Roger, I. Dez, Hydrophobization of chitosan films by surface grafting with fluorinated polymer brushes, Carbohydr. Polym. 205 (2019) 437-446. https://doi.org/10.1016/j.carbpol.2018.10.044.

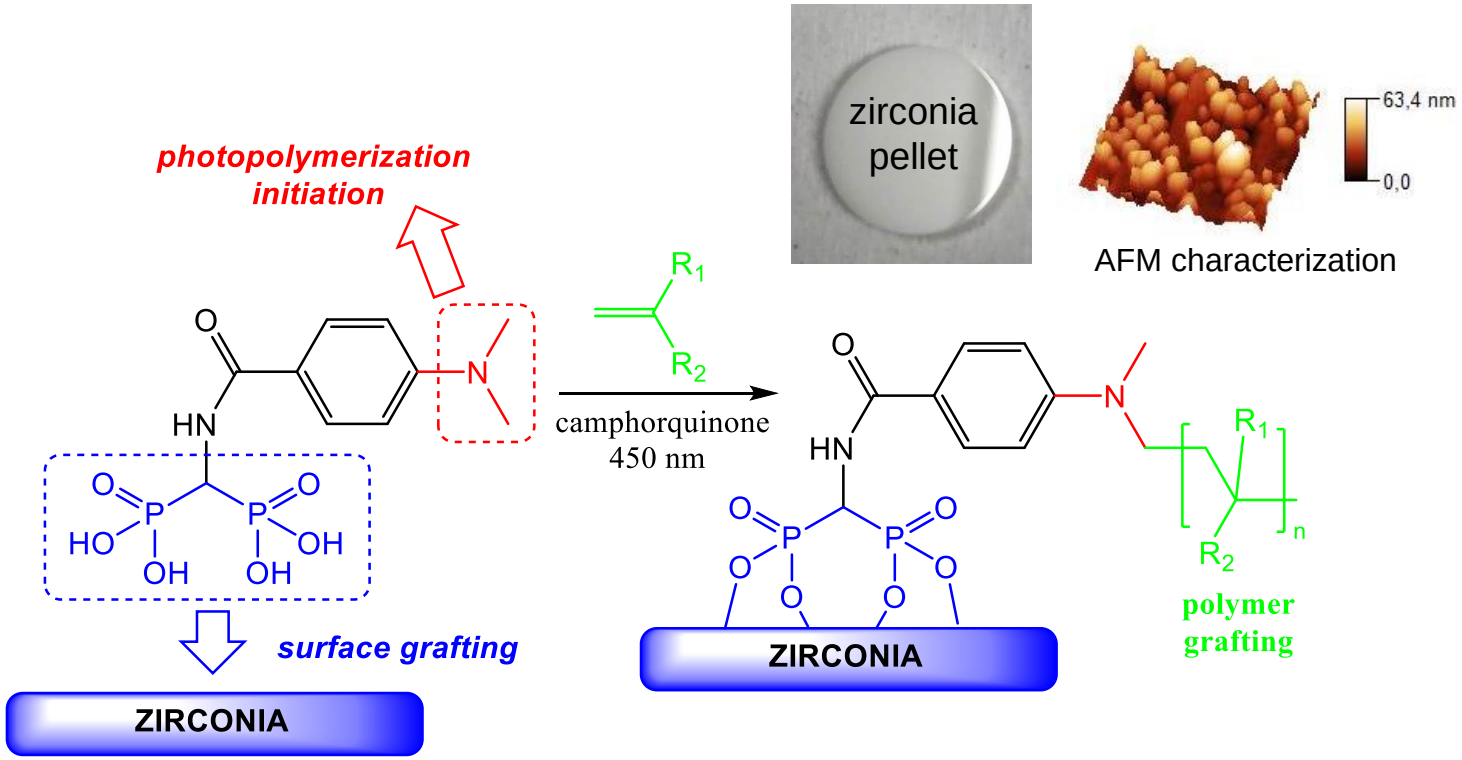
zirconia pellet
63,4 nm
0,0
AFM characterization
photopolymerization initiation
camphorquinone
450 nm
surface grafting
ZIRCONIA
ZIRCONIA
polymer grafting